

Cobalt Modified N-doped Carbon Nanotubes for Catalytic C=C Bond Formation via Dehydrogenative Coupling of Benzyl Alcohols and DMSO

Jinlei Li^{‡,§,†}, Guoliang Liu^{‡,†}, Lijun Shi^{‡,§}, Qi Xing[‡], Fuwei Li^{‡,*}

[‡]State Key Laboratory for Oxo Synthesis and Selective Oxidation, Suzhou Research Institute of LICP, Lanzhou Institute of Chemical Physics (LICP), Chinese Academy of Sciences, Lanzhou 730000, P. R. China

[§]University of Chinese Academy of Sciences, Beijing 100049, P. R. China

†Author contributions:

These authors contributed equally.

***Corresponding authors:**

Email:

fuweili@licp.cas.cn

Table of Contents

1. General remarks
2. General procedures
 - 2.1. Procedure for the preparation of Co@NCNT
 - 2.2. General procedures for the dehydrogenation reactions
3. Characterization of Co@NCNT
 - 3.1 TEM and SEM images of Co@NCNT-700, -800 and -900
 - 3.2 N₂ adsorption–desorption isotherm and BET surface areas of various samples
 - 3.3 XPS spectra of Co@NCNT samples
4. Experiment procedures
 - 4.1. Optimization of reaction conditions
 - 4.2 Heterogeneity nature of the reaction by a hot filtration test
 - 4.3 Relationship of the nitrogen content and graphitic degree with the catalytic performance
 - 4.4 Mechanistic investigations
 - 4.4.1 Evidence of the source for and the release of H₂
 - 4.4.2 Identification of the active sites by KSCN poisoning test
 - 4.4.3 Investigation of reaction mechanism
 - 4.4.4 Deuterium-labeling experiments
 - 4.4.5 Investigation of possible reaction intermediate using different reactants
 - 4.4.6 Identification of reaction intermediate by time-course study
 - 4.4.7 Identification of reaction intermediate by control experiment with styryl sulfoxide
 - 4.4.8 Identification of the reduction of styryl sulfoxide in a non-radical pathway
 - 4.5 Characterization of the used catalyst using TEM and XRD
 - 4.6 The procedure for the synthesis of intermediate
5. References
6. NMR spectra

1. General remarks

All reagents were purchased from commercial sources (TCI, Alfa Aesar, Acros, Energy Chemical, Zhongkekaite Sci-Tech & Industry Trade Co., Ltd) and used directly without further purification. Ar, O₂ and N₂ used in this work are of high purity (99.999%) provided by Lanzhou Zhongkekaite Sci-Tech & Industry Trade Co., Ltd.

Unless otherwise noted, all reactions were performed in a 50 mL Schlenk glass tube with a magnetic bar. The pyrolysis procedure was carried out in a GSL-1500X tubular furnace provided by Hefei Kejing Materials Technology Co., Ltd.

¹H and ¹³C NMR spectra were recorded on a Bruker 400 MHz spectrometer and all chemical shifts were given in parts per million (ppm) relative to the standard tetramethylsilane (0.00 ppm for ¹H NMR in CDCl₃) and d-solvent peaks ($\delta = 77.16$ for ¹³C NMR, chloroform), respectively.

Powder X-ray diffraction (XRD) patterns were recorded on a PANalytical X-ray diffractometer with a Cu K α ($\lambda=1.5418$ Å) radiation source. Phase identification was made by using the PDF-2 database of the International Center of Diffraction Data (ICDD).

X-ray photoelectron spectroscopy (XPS) was performed on a Thermo Scientific ESCALAB 250Xi Spectrometer with a monochromatic X-ray source. All of the binding energies were calibrated by using the adventitious carbon (C1s =284.8 eV) as a reference.

Transmission electron microscopy (TEM) was performed on a FEI JEM-1200-EX electron microscope operated at an acceleration voltage of 200 kV. TEM samples were prepared by placing a droplet of catalyst dispersion onto a holey carbon film on a Cu grid.

Raman spectra were measured by using a LabRam HR800 spectrometer (HORIBA Jobin Yvon) equipped with a 532 nm excitation laser at room temperature.

N₂ adsorption-desorption experiments were carried out on an ASAP 2020 Micromeritics Instrument at 77 K. Each sample was degassed at 180 °C for 4 hours before the measurement. The specific surface area was calculated from the adsorption data using the Brunauer-Emmett-Teller (BET) method and the pore size distributions were obtained from the desorption branch isotherms using the BJH (Barrett–Joyner–Halenda) method.

2. General procedures

2.1 General procedure for the preparation of Co@NCNT

The catalysts were prepared using a facile thermal pyrolysis. In a typical process, a mixture of $\text{Co}(\text{NO}_3)_2 \cdot 6\text{H}_2\text{O}$ (9.23 g, 31.7 mmol), glucose (1 g), and melamine (40 g, 317 mmol) was pyrolyzed under N_2 atmosphere. The mixture was first heated to 600 °C at a heating rate of 2.5 °C min^{-1} and hold for another 2 h. Then the temperature was raised to the desired temperature at a heating rate of 3.3 °C min^{-1} and hold for 1 h. The obtained powder was denoted as Co@NCNT-*x*, where *x* represents the final pyrolysis temperature (700, 800 and 900 °C). In addition, $\text{CoCl}_2 \cdot 6\text{H}_2\text{O}$ and $\text{Co}(\text{CH}_3\text{COO})_2 \cdot 4\text{H}_2\text{O}$ were also used as the metal precursors to prepare the Co@NCNT catalysts, which denoted as Co@NCNT-800-Cl and Co@NCNT-800-Ac, respectively. For comparison, we also prepared carbon supported Co (denoted as Co@C) and N-doped carbon (denoted as NC) by using mixed precursors without melamine and metal source, respectively. The Co/NAC catalyst was prepared via a post-deposition method with $\text{Co}(\text{NO}_3)_2 \cdot 6\text{H}_2\text{O}$ as the metal source and N-doped activated carbon as the support. The Co/NAC sample was reduced under high-purity H_2 atmosphere at 400 °C for 2 h to ensure Co in metallic state.

2.2 General procedures for the dehydrogenation reactions

Catalytic tests were carried out in a 50 mL Schlenk glass tube with a magnetic stirring bar. In a typical reaction, benzyl alcohol (1 mmol, 108 mg), DMSO (3 mmol, 234 mg), KO^tBu (20 mol%, 22.4 mg), Co@NCNT-800 (9 mol%, 20 mg), *n*-dodecane (100 mg) as the internal standard and toluene (2 mL) as the solvent were mixed in the glass test tube. The tube was then sealed and purged with N_2 three times before it was finally pressurized to 1.0 bar. Subsequently, the reaction mixture was vigorously stirred at the desired temperature for the specific reaction time. After cooling to room temperature, excess N_2 was released and then the catalyst was collected via magnetic separation. Finally, the resultant product mixtures were determined by gas chromatography/mass spectrometry (GC-MS, Agilent 7890A/5975C) and analyzed on GC (Agilent 7890A) equipped with a SE-54 column and a flame ionization detector (FID).

For the reuse of Co@NCNT-800, the reaction was performed with 1 mmol of benzyl alcohol, 3 mmol of DMSO, 20 mol% of KO^tBu, 20 mg of Co@NCNT-800, 100 mg internal standard *n*-dodecane and 2 mL of toluene at 160 °C under N_2

protection for 12 h. After each cycle, Co@NCNT-800 was collected by magnetic separation and washed several times with ethanol and water, followed by vacuum drying at 80 °C for 12 h. There is no re-activation procedure for each cycle.

For the detection of H₂, the test tube was cooled to room temperature when the reaction was stopped. And the upper gas was collected by a syringe from the branch of the test tube. Then the collected gas was analyzed by GC and GC/MS with a thermal conductivity detector (TCD) using N₂ and Ar as the carrier gas, respectively.

3 Characterization of Co@NCNT

3.1 TEM and SEM images of Co@NCNT-700, -800, and -900.

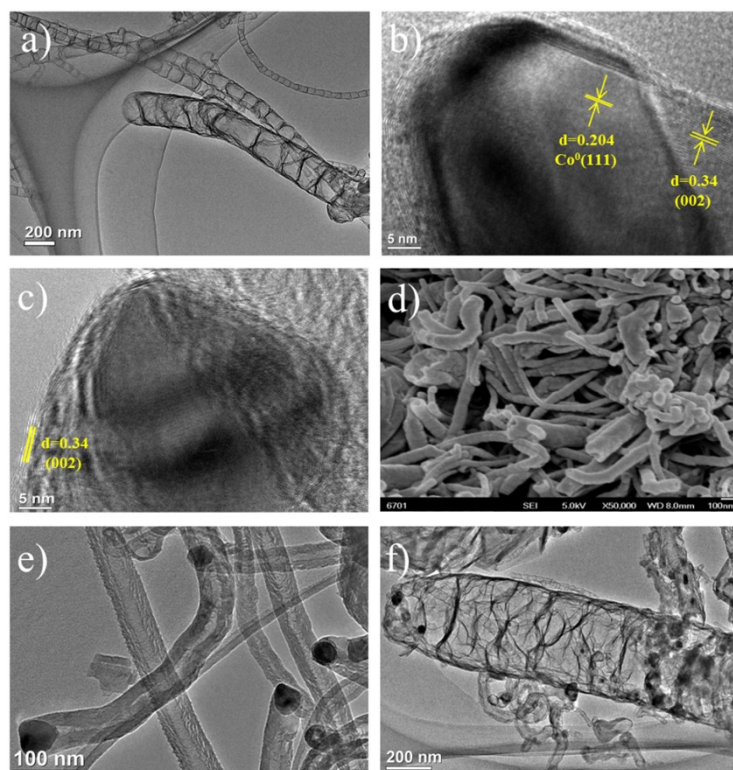


Figure S1 a-c) TEM and d) SEM images of Co@NCNT-800 and TEM images of e) Co@NCNT-700 and f) Co@NCNT-900.

TEM images of Co@NCNT-800 shows bamboo-like nanotubes with metallic Co NPs inside them (**Figure S1a**). Detailed analysis using HR-TEM shows that Co NPs are wrapped by graphene layers (**Figures S1b** and **1c**). The SEM image features with different diameters from 30 to 200 nm (**Figure S1d**). Co@NCNT-700 and Co@NCNT-900 display very similar carbon nanotube structures to that of Co@NCNT-800 (**Figures S1e** and **1f**).

3.2 N₂ adsorption–desorption isotherm and BET surface areas of various samples

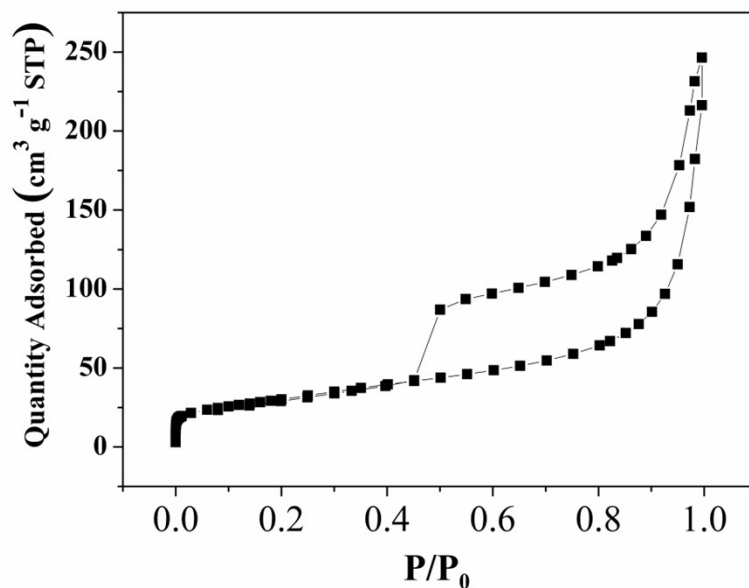


Figure S2 N₂ adsorption–desorption isotherm of Co@NCNT-800.

Table S1 BET surface areas of the samples.

Sample	S_{BET} (m ² g ⁻¹)
NC	560
Co@C	17
Co@NCNT-700	106
Co@NCNT-800	102
Co@NCNT-900	95
NAC	1124
Co/NAC	1208

The N₂ adsorption–desorption isotherm of Co@NCNT-800 in **Figure S2** illustrates a distinct hysteresis loop at the relative pressure P/P₀ ranging from 0.45 to 1.0, indicative of abundant meso-/macro-pores. The Brunauer–Emmett–Teller (BET) surface areas of Co@NCNT-700, -800 and -900 are very close (95–106 m² g⁻¹), but much lower than that of the Co-free NC sample (560 m² g⁻¹).

3.3 XPS spectra of the Co@NCNT samples

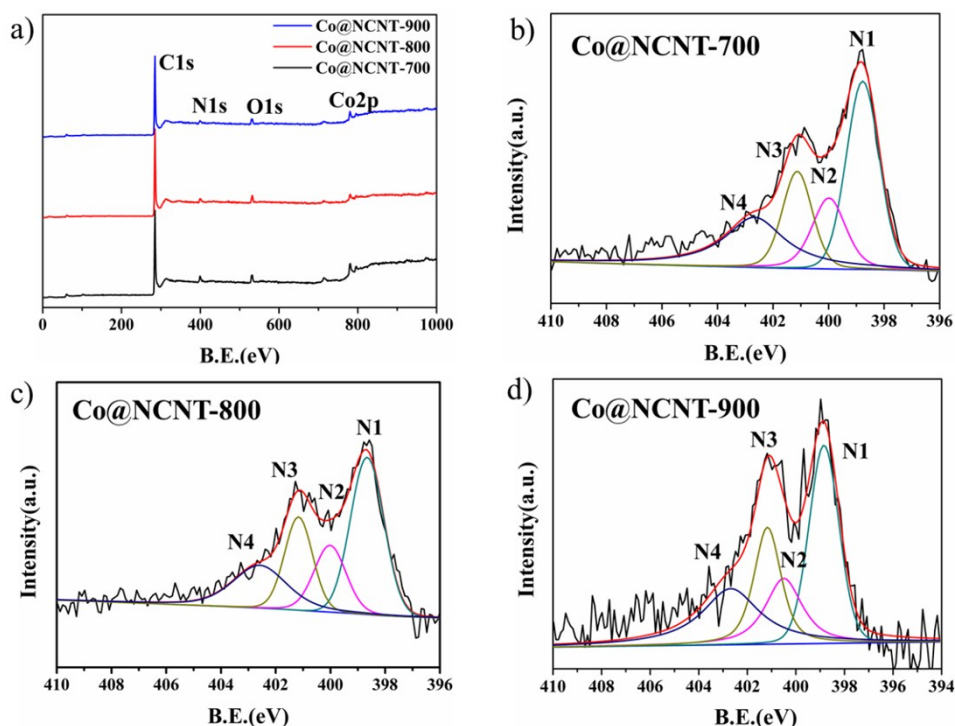


Figure S3 a) XPS survey spectra and b-d) high resolution scans of N 1s for different Co@NCNT samples.

Figure S3 presents the survey spectra of Co@NCNT-700, -800 and -900, with characteristic spectra of C 1s (285.3 eV), N 1s (399.6 eV), O 1s (532.6 eV) and Co 2p (781.1 eV). All Co@NCNT samples possess four types of nitrogen species including pyridinic N (N1), pyrrolic N (N2), quaternary N (N3) and oxidized-N (N4) species.

Table S2 N-species of NC and Co@NCNT samples obtained by XPS.

Sample	N1	N2	N3	N4	N content (atom%)
NC	48%	19%	19%	14%	8.9
Co@NCNT-700	38%	16%	19%	27%	5.7
Co@NCNT-800	40%	17%	21%	21%	4.1
Co@NCNT-900	34%	18%	22%	26%	3.8

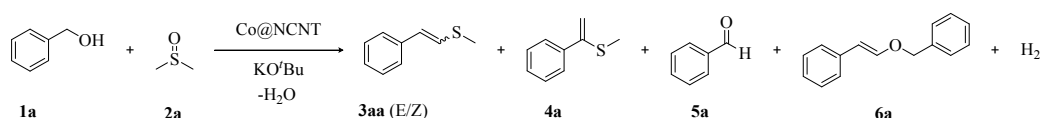
N1: pyridinic N, **N2:** pyrrolic N, **N3:** quaternary N, **N4:** oxidized N.

4. Experimental procedures

4.1 Optimization of reaction conditions

To optimize the reaction conditions, we studied the molar ratio of benzyl alcohol to DMSO, base amount, solvent, reaction time, and reaction temperature in the direct dehydrogenative coupling reaction of benzyl alcohol (**1a**) with DMSO over the Co@NCNT-800 catalyst.

Table S3 Optimization of reaction conditions - molar ratio of **1a** to DMSO^{a,b}.



Entry	Molar ratio of 1a to DMSO	Conversion of 1a (%)	Yield of 3aa (E/Z) (%)	Yield of 4a (%)	Yield of 5a (%)	Yield of 6a (%)
1	1:2	76	46 (79/21)	6	2	8
2	1:3	78	57 (82/18)	3	2	10
3	1:4	63	36 (85/15)	5	1	11

^aReaction conditions: catalyst 20 mg (9 mol% Co), **1a** 1 mmol, DMSO x mmol (x=2, 3, 4), KO^tBu 56 mg (50 mol%), toluene 2 mL, N₂, 150 °C, 24 h. ^bThe yields was based on GC with dodecane as internal standard.

We first carried out the reaction at different molar ratios of **1a** to DMSO. As shown in **Table S3**, when the molar ratio of **1a** to DMSO was 1:3, we obtained the highest catalytic activity (78% conversion of **1a** and 57% yield of **3aa**). Therefore, we chose 1:3 of the molar ratio of **1a** to DMSO for further optimization of other parameters.

Table S4 Optimization of reaction conditions - **base amount**^{a,b}.

Entry	Base amount (mol%)	Conversion of 1a (%)	Yield of 3aa (E/Z) (%)	Yield of 4a (%)	Yield of 5a (%)	Yield of 6a (%)
1	10	58	23 (74/26)	3	6	1
2	20	73	59 (83/17)	7	2	6
3	50	78	57 (82/18)	3	2	10
4	100	78	36 (87/13)	4	ND	7
5	200	89	7 (100/0)	ND	ND	5
6 ^c	20	63	40 (77/23)	6	5	9
7 ^d	20	16	ND	ND	15	ND

^a Reaction conditions: Co@NC-800 20 mg (9 mol% Co), **1a** 1 mmol, DMSO 3 mmol, KO^tBu (x mol%) (x=10, 20, 50, 100, 200), toluene 2 mL, N₂, 150 °C, 24 h. ^b The yields was based on GC with dodecane as internal standard. ^c KOH. ^d K₂CO₃. ND: not detected.

In the previous reports, a proper amount of base was normally required to assist the activation of O-H or C-H bonds of reactants. To realize the formation of styryl sulfides, traditional routes require equivalent or even excess base. However, in this work, a catalytic amount of KO^tBu (20 mol%) was able to realize the highest yield of **3aa** (65%), as shown in **Table S4**. A further increase of the base amount had no promotion or even decreased the yield of **3aa**. Notably, when the base amount was increased to 200 mol%, the titled reaction was significantly inhibited, with only 7% yield of **3aa**. This demonstrated that the base amount played an important role in the catalysis.

Furthermore, other bases such as KOH, K₂CO₃ were also tested in the reaction. KOH involved system showed a similar conversion (63%) of **1a** with the KO^tBu system but the **3aa** yield was a bit lower (40%). When K₂CO₃ was used instead of KO^tBu, no formation of **3aa** was obtained, which illustrated that the titled reaction requires a strong base. From above analyses, the catalytic performance of our reaction was determined by both the dosing amount and type of base. At last, we chose 20 mol% of KO^tBu as the best choice to perform the further investigations.

Table S5 Optimization of reaction conditions – solvent^{a,b}.

Entry	Solvent	Conversion of 1a (%)	Yield of 3aa (E/Z) (%)	Yield of 4a (%)	Yield of 5a (%)	Yield of 6a (%)
1	toluene	73	59 (83/17)	7	2	6
2	xylene	63	45 (81/19)	6	4	5
3	nonane	89	52 (79/21)	5	2	7
4	THF	44	36 (84/16)	4	0	4
5	acetonitrile	0	0	0	0	0
6	dioxane	31	18 (84/16)	2	3	5

^a Reaction conditions: Co@NC-800 20 mg (9 mol% Co), **1a** 1 mmol, DMSO 3 mmol, KOtBu 22.4 mg (20 mol%), solvent 2 mL, N₂, 150 °C, 24 h. ^b The yields was based on GC with dodecane as internal standard.

Solvent normally plays an important role in heterogeneous catalysis. In this work, we tested several solvents including toluene, p-xylene, nonane, tetrahydrofuran (THF), acetonitrile and dioxane in the reaction of **1a** with DMSO. As presented in **Table S5**, we got a moderately high conversion of **1a** but the highest yield of **3aa** in toluene (73% and 59%, entry 1). Although the highest conversion of **1a** (89%) was obtained in nonane, but the yield of **3aa** was only 52% with poor selectivity, inferior to that in toluene as solvent. Other solvents such as THF, dioxane and acetonitrile disfavor the formation of **3aa**. Note that there was no formation of **3aa** in acetonitrile, but a byproduct 2,6-dimethylpyrimidin-4-amine via the polymerization of acetonitrile was formed instead. Therefore, in terms of the yield of **3aa**, we chose toluene as the best solvent for further optimization.

Table S6 Optimization of reaction conditions – **reaction time**^{a,b}.

Entry	t(h)	Conversion of 1a (%)	Yield of 3aa (E/Z) (%)	Yield of 4a (%)	Yield of 5a (%)	Yield of 6a (%)
1	8	54	41 (79/21)	5	1	6
2	12	63	51 (82/18)	6	2	4
3	16	70	54 (82/18)	7	2	6
4	24	73	59 (82/18)	7	2	6

^a Reaction conditions: Co@NC-800 20 mg (9 mol% Co), **1a** 1 mmol, DMSO 3 mmol, KOtBu 22.4 mg (20 mol%), toluene 2 mL, N₂, 150 °C, t h. ^bThe yields was based on GC with dodecane as internal standard.

Conversion and selectivity was both changed with reaction time and it is desired to find the balance between the conversion/selectivity and the reaction time. Therefore, we performed the reaction with different reaction time, and the results were shown in **Table S6**. We found that the conversion changed slowly after 16 h, and the highest selectivity of **3aa** (81%) was obtained at 12 h. So, we chose 12 h as the reaction time to continue the further investigations.

Table S7 Optimization of reaction conditions – **temperature**^{a,b}.

Entry	T(°C)	Conversion of 1a (%)	Yield of 3aa (E/Z) (%)	Yield of 4a (%)	Yield of 5a (%)	Yield of 6a (%)
1	120	23	19 (61/39)	2	0.5	2
2	130	43	35 (70/30)	4	1	3
3	140	63	51(76/24)	6	1	6
4	150	63	51 (82/18)	6	2	4
5	160	92	76 (85/15)	6	2	7
6	170	96	74 (86/14)	10	5	7

^a Reaction conditions: Co@NC-800 20 mg (9 mol% Co), **1a** 1 mmol, DMSO 3 mmol, KOtBu 22.4 mg (20 mol%), toluene 2 mL, N₂, T °C, 12 h. ^b The yields was based on GC with dodecane as internal standard.

Reaction temperature was another important factor, which can change the extent of the reaction and thus influence the catalytic performance. As the titled reaction was an entropy increase reaction, therefore, increasing the reaction temperature could facilitate the reaction to some extent. As we expected, from the results shown in **Table S7**, the conversion increased with the increase of the reaction temperature

while the selectivity changed slowly. As the highest yield of **3aa** was obtained at 160 °C, we chose 160 °C as the reaction temperature for further studies.

4.2 Heterogeneity nature of the reaction by a hot filtration test

A hot filtration test was carried out to verify the nature of “heterogeneity” of the reaction. The Co@NCNT-800 catalyst was removed from the catalytic system when the reactions proceed at a **1a** conversion of 37% and then the reaction was restarted for another 2 h. The result showed that no further **3aa** was produced after the Co@NCNT-800 catalyst was filtered off, indicating the true heterogeneity nature of Co@NCNT catalyst.

4.3 Relationship of the nitrogen content and graphitic degree with the catalytic performance

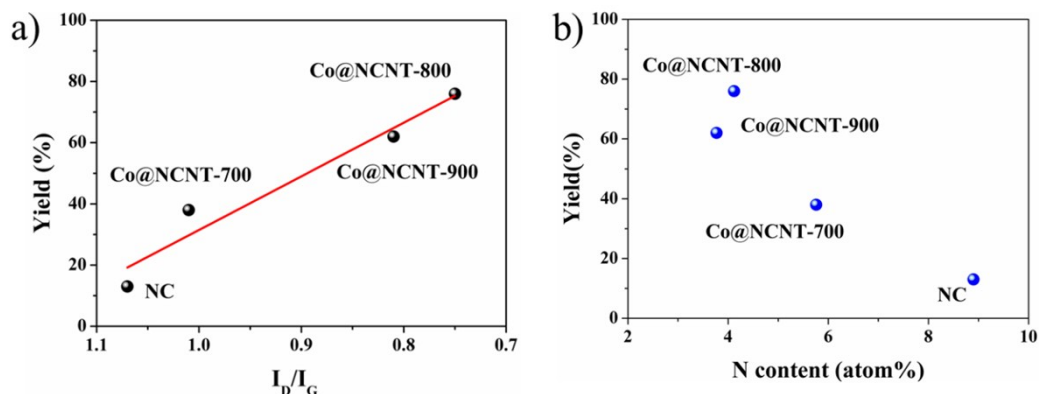


Figure S4 The relationship between the **3aa** yield and a) I_G/I_D ratio and b) N content.

When the **3aa** yield was correlated with the I_D/I_G value, we clearly find a nearly linear relationship in **Figure S4**. A high graphitization degree (low I_D/I_G) would favor the **3aa** synthesis.

Traditionally, N species also played an important role in the catalytic performance in electrochemical reactions and the fine chemical synthesis reactions catalyzed by M-N-C or N-doped carbon catalysts. In this work, after we carefully examined the nitrogen content in NC, Co@NCNT-700, -800 and -900 catalysts (**Table S2**), there seems no direct correlation between N content and catalytic performance.

In general, the surface area also plays an important role in the catalytic performance. However, the surface area also displayed a non-linear relationship. Co@NCNT-700, -800, -900 show very similar surface area ($95\text{--}106\text{ m}^2\text{ g}^{-1}$) which is much lower than that of NC ($560\text{ m}^2\text{ g}^{-1}$), while the activity was decrease in the following order Co@NCNT-800 > Co@NCNT-900 > Co@NCNT-700 > NC.

4.4 Mechanistic investigations

4.4.1 Evidence of the source for and the release of H_2

We detected the release of H_2 in the titled reaction via GC-MS. To found out the source of the released H_2 , we first used DMSO-*d*6 instead of DMSO to check out if DMSO was a possible H_2 source. As shown in **Figure S5**, the signals of D_2 , HD and H_2 were observed, indicating that both DMSO-*d*6 and **1a** were sources for H_2 release.

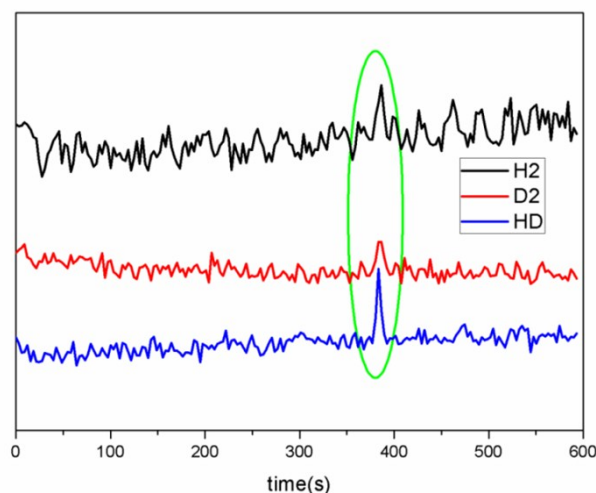
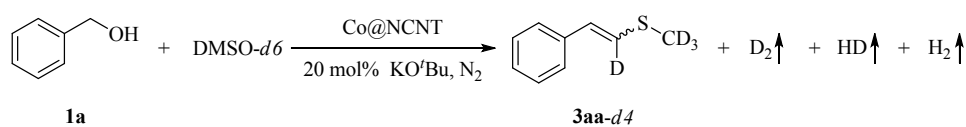


Figure S5 GC-MS signal for the source of H₂ release in the reaction of **1a** and DMSO-*d*₆.

Reaction conditions: **1a** 1 mmol, DMSO-*d*₆ 3 mmol, Co@NCNT-800 20 mg (9 mol%),
 KO^tBu 22.4 mg (20 mol%), N₂, 160 °C, 12 h.

To explore the dehydrogenation of substrates, we performed control experiments by using **1a** and DMSO as the sole reactant with and without the Co@NCNT-800 catalyst. The detection of H₂ release was shown in **Figure S6**. We could find the H₂ release in all reactions whether with or without Co@NCNT-800, but the amount of H₂ was different. In the **1a** system, the intensity of H₂ release could be improved by around 3 times from 6.65E-008 to 2.10E-007 after the use of Co@NCNT-800 (**Figures S6a** and **6b**). This demonstrated that Co@NCNT-800 can promote the dehydrogenation of **1a**. In the DMSO system, nearly no obvious change in H₂ amount was obtained, suggesting a non-catalyzed process. Moreover, when we compared the two systems with Co@NCNT-800 as catalyst, we found that the amount of H₂ release in the **1a** system is much larger than that in the DMSO system. This indicates that the H₂ is mainly released from the dehydrogenation of benzyl alcohol.

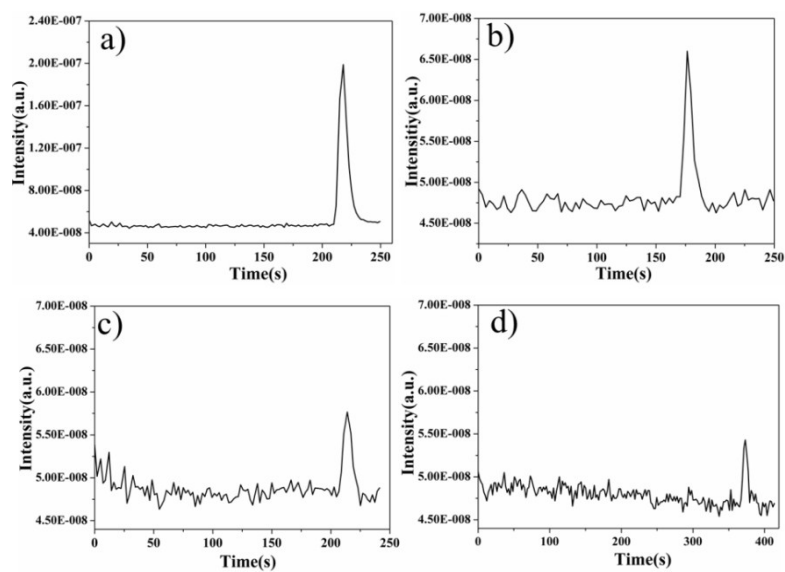


Figure S6 GC-MS signal for the release of H₂ by **1a** or DMSO with or without Co@NCNT catalyst respectively. **1a** a) with and b) without Co@NCNT-800; DMSO c) with and without d) Co@NCNT-800 Reaction conditions: **1a** 1 mmol, DMSO 3 mmol, Co@NCNT-800 20 mg (9 mol%), KO^tBu 22.4 mg (20 mol%), N₂, 160 °C, 12 h.

4.4.2 Identification of the active sites by KSCN poisoning test

We carried out the poisoning tests with KSCN involved in the reactions, as SCN⁻ ions have strong affinity to surface Co. The amount of KSCN was equal to 16 equivalents (equiv.) of the Co amount used in the reaction system. Perhaps one may doubt that whether 16 equiv. of KSCN could block the overall cobalt sites or not, we then carried out a similar poisoning test in the hydrogenation of quinoline over Co@NCNT-800. As shown in **Figure S7**, we found that when the reaction was carried out without KSCN, 76% conversion of quinoline was obtained, with 97% selectively to 1,2,3,4-tetrahydroquinoline. However, no reaction happened when the reaction was performed with 16 equiv. of KSCN (**Figure S7**). This demonstrated that 16 equiv. of KSCN was able to poison the overall cobalt surface. As for our reaction, shown in **Figure 2a** in the Main text, we can clearly find that KSCN had very limited negative influence on the catalytic performance, with the decrease in **1a** conversion from 92% to 84% while the **3aa** yield displayed an obviously decrease from 76% to 53%. So we conclude that surface Co sites were not active sites. Based on our control experiments in **Table 1** in the main text, we are convinced that NCNTs provide active sites for the dehydrogenative coupling reaction while the Co nanoparticles were regarded as an electron modifier via strong metal-NCNT interactions rather than a spectator.

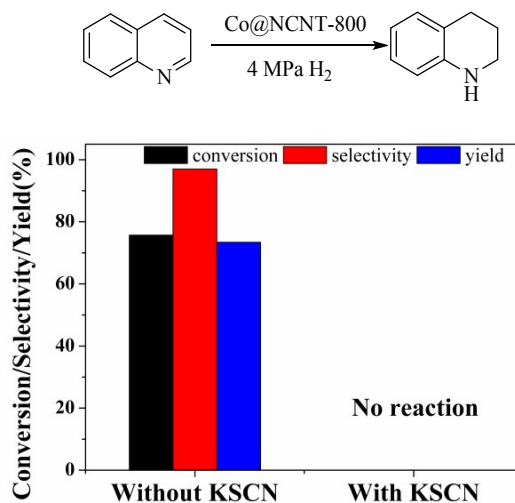
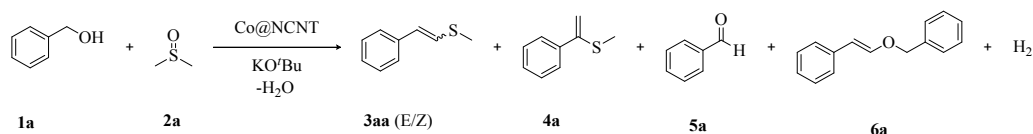


Figure S7 Poisoning test of the Co@NCNT-800 catalyst with KSCN in the hydrogenation of quinoline.

4.4.3 Investigation of reaction mechanism

Table S8 Investigation of reaction mechanism by radical-trapping experiments^{a,b}.



Entry	Additive	Conversion of 1a (%) ^c	Yield of 3aa (E/Z) (%)	Yield of 4a (%)	Yield of 5a (%)	Yield of 6a (%)
1	-	92	76 (85/15)	6	2	7
2 ^d	-	81	0	0	72	0
3	TEMPO	84	3 (67/33)	1	67	0
4 ^e	TEMPO	79	66 (77/23)	8	N.D.	5
5	BQ	35	0	0	8	N.D.
6	DPE	84	68 (81/19)	9	5	6
7	BHT	62	43 (74/26)	7	2	4
8 ^f	-	84	68 (84/16)	9	N.D.	8

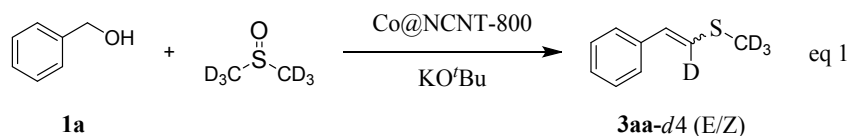
^a Reaction conditions: Co@NCNT-800 20 mg (9 mol% Co), **1a** 1 mmol, DMSO 3 mmol, KOtBu 22.4 mg (20 mol%), additive (1 equiv.), toluene 2 mL, N₂, 160 °C, 12 h. ^b The yields was based on GC with dodecane as internal standard. ^c Conversion was obtained by using GC. ^dO₂. ^e0.2 equiv. TEMPO was used. ^fH₂. N.D.: not detected.

To check if any radical intermediates were involved in the reaction, we investigated several conventional radical scavengers such as 2,2,6,6-tetramethylpiperidiny-1-oxide (TEMPO), 2,6-di-tert-butyl-4-methylphenol (BHT), 1,1-Diphenylethylene (DPE), 1,4-benzoquinone (BQ). Surprisingly, the formation of **3aa** was significantly suppressed when TEMPO and BQ (1 equiv.) was introduced into the reaction, respectively (entries 3 and 5, **Table S8**). By contrast, when DPE was used as the radical scavenger, both **1a** conversion and **3aa** yield were comparable to that without a radical scavenger (84% vs 92%, 68% vs 76% entries 6 and 1, **Table S8**). Also, the BHT system still showed an acceptable **3aa** yield of 43% due to a slight decrease in the selectivity of **3aa** (69% vs 83%, entries 5 and 1, **Table S8**). These results suggest that the reaction is not experiencing a radical pathway. But the interesting thing is that the radical scavengers with oxidative character could inhibit the formation of **3aa** while the others have marginal effect on the synthesis of **3aa**. To further confirm this aspect, we reduced the amount of TEMPO (0.2 equiv.) and 66% yield of **3aa** was obtained (entry 4, **Table S8**), which is comparable to that of the

standard condition (entry 1, **Table S8**). Moreover, a reduced product TEMPOH was observed by GC-MS. Therefore, we believed that the TEMPO and BQ may lead to the similar reaction pathway as that with O₂ where the reaction was stopped at the stage of **5a** (entries 2, 3 and 5, **Table S8**). We then performed the reaction under a reducible H₂ atmosphere and 68% yield of **3aa** was obtained (entry 7, **Table S8**), which is comparable to that in N₂ (entry 1, **Table S8**). This also indicated the negative role of oxidizing agents in the C-C coupling reaction.

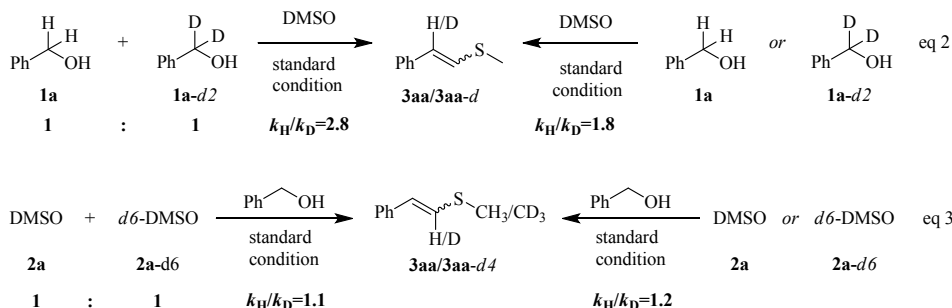
4.4.4 Deuterium-Labeling experiments

To support DMSO as the direct olefination agent, we use DMSO-*d*6 to react with **1a** to synthesize styryl sulfide (eq 1). ¹H NMR clearly showed the almost 100% deuterium incorporation at the bridged carbon between C=C and C-S bonds as well as the terminated methyl group.



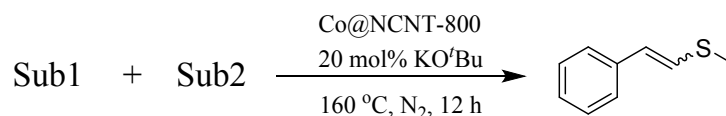
To shed light on the mechanism of the reaction, we performed the deuterium-labeling experiments with benzyl alcohol-*d*2 (**1a-d**2) or DMSO-*d*6 as the reactant to investigate the kinetic isotope effects (KIE) of the reaction under the standard reaction condition. As shown in eq 2, by using **1a** and **1a-d**2 to react with DMSO in parallel experiments, we obtained the reaction rate ratio ($k_{\text{H}}/k_{\text{D}}$) of 1.8. This indicates that the cleavage of the C–H bond is a moderately slow step. On the other hand, the intermolecular competition experiment using equimolar amounts of **1a** and **1a-d**2 was also carried out. ¹H NMR analysis of the product mixture gave a **3aa**/**3aa-d** molar ratio of 2.8. The two KIE values greatly supported C-H cleavage of benzyl alcohol as the rate-determining step.

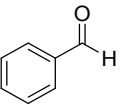
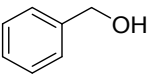
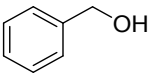
In addition, we performed the parallel experiments and intermolecular completion experiments by using DMSO and DMSO-*d*6 to react with benzyl alcohol to investigate the KIE under the standard condition. As shown in eq 3, the two KIE values were very close (1.2 and 1.1). No significant isotope effects were observed. This indicates that the cleavage of C-H of DMSO did not involve in the rate limiting-step.



4.4.5 Investigation of possible reaction intermediate using different reactants

Table S9 Control experiments with different starting reactants^{a,b}.



Entry	Sub1	Sub2	Yield of 3aa (%)
1		DMSO	N.D.
2		DMS	N.D.
3		dimethyl sulfone	N.D.

^a Reaction conditions: Co@NCNT-800 20 mg (9 mol% Co), **Sub 1** 1 mmol, **Sub 2** 3 mmol DMSO, KO^tBu 20 mg (20 mol%), toluene 2 mL, N₂, 160 °C, 12 h. ^b The yields was based on GC with dodecane as internal standard.

Generally, DMSO would undergo a slow disproportionation to give dimethyl sulfide (DMS) and dimethyl sulfone under a high temperature condition. Actually, DMS was detected by GC-MS in our system. When we replaced DMSO with DMS or dimethyl sulfone (entries 2 and 3, **Table S9**), no yield of **3aa** was obtained in both reactions. Therefore, it is believed that DMSO must directly react with the above adsorbed aldehyde intermediate in the second step. Time-interval reaction analyses unveiled a transient intermediate, which was identified as styryl sulfoxide by GC-MS and NMR. Meanwhile, styryl sulfoxide was thought as an important intermediate for the synthesis of styryl ether from **1a** and DMSO under aerobic condition in the previous report by Zhang et.al.¹

4.4.6 Identification of reaction intermediates by time-course study

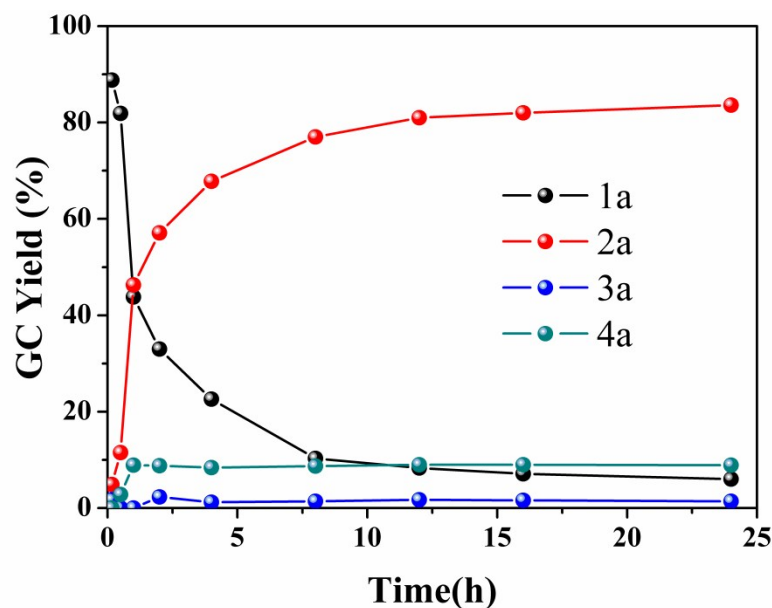
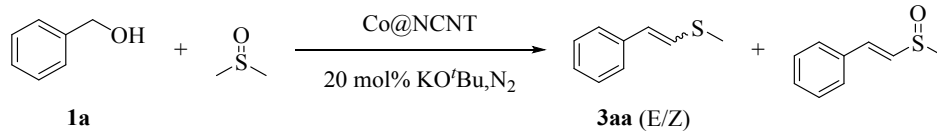


Figure S8 Time course of the coupling reaction of benzyl alcohol and DMSO over Co@NCNT-800. Reaction conditions: Co@NCNT-800 20 mg (9 mol% Co), **1a** 1 mmol, DMSO 3 mmol, KO^tBu 22.4 mg (20 mol%), toluene 2 mL, N₂, 160 °C.

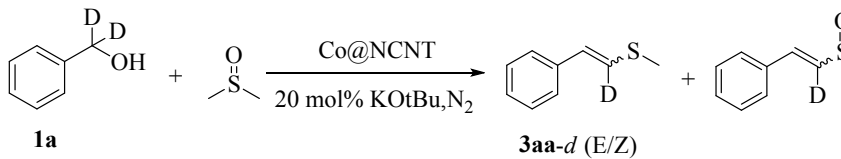
Time-interval experiments were conducted to study the reaction mechanism on the dehydrogenative coupling of benzyl alcohol and DMSO over Co@NCNT-800 (**Figure S8**). The conversion of **1a** and the yield of different products were determined by gas chromatography. We did not find any reaction intermediates under the standard reaction. So, we decided to perform the reaction under a lower temperature (130 °C) to find some clues for the reaction intermediates. The results were shown in **Table S10**.

Table S10 Investigation of the possible reaction intermediate by time course study at 130 °C^{a,b}.



Time (min)	Conversion of 1a (%)	Yield of styryl sulfoxide (%)	Yield of 3aa (E/Z) (%)
20	11	0.4	3.2 (74/26)
40	19	ND	6.5 (73/27)
60	28	ND	10.9 (74/26)

^a Reaction conditions: Co@NCNT-800 10 mg (9 mol% Co), **1a** 0.5 mmol, DMSO 1.5 mmol, KO^tBu 22.4 mg (20 mol%), toluene 1 mL, N₂, 130 °C, t min. ND: not detected. ^b The yields was based on GC with dodecane as internal standard.



Time (min)	Conversion of 1a (%)	Yield of styryl sulfoxide (%)	Yield of 3aa-d (E/Z) (%)
20	9	0.7	ND
40	16	3.4	ND
60	24	ND	8.4 (74/26)

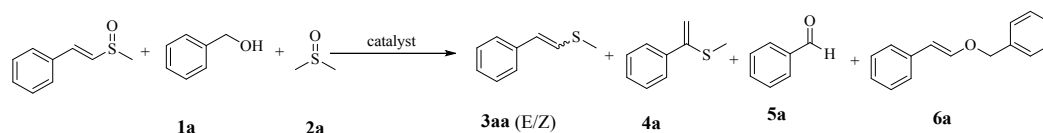
^a Reaction conditions: Co@NCNT-800 10 mg (9 mol% Co), **1a** -d₂ 0.5 mmol, DMSO 1.5 mmol, KO^tBu 22.4 mg (20 mol%), toluene 1 mL, N₂, 130 °C, t min. ^b The yields was based on GC with dodecane as internal standard.

We performed the reaction at 130 °C. At the initial stage, we detected a very trace amount of the styryl sulfoxide (0.4% of yield) in 20-min reaction. It disappeared very quickly when the reaction proceeded for 40 and 60 min. The fast conversion of styryl sulfoxide to the final **3aa** can explain the fact of no detectable intermediate for a reaction at 160 °C. Moreover, the deuterium-labeling time-course tests by using d₂-benzyl alcohol (**1a-d₂**) also confirmed the presence of styryl sulfoxide with a yield of 0.7% and 3.4% at a reaction time of 20 and 40 min, respectively. The slightly increased amount of styryl sulfoxide is due to the decrease of the total reaction rate.

Therefore, we believed styryl sulfoxide as an important intermediate. We next employed styryl sulfoxide as the starting reactant to verify whether it could be converted to the desired product under the standard condition. The results and related discussions were shown in the next part 4.2.8.

4.4.7 Identification of reaction intermediate by control experiment with styryl sulfoxide

Table S11 Control experiments with styryl sulfoxide as a starting substrate^{a,b}.



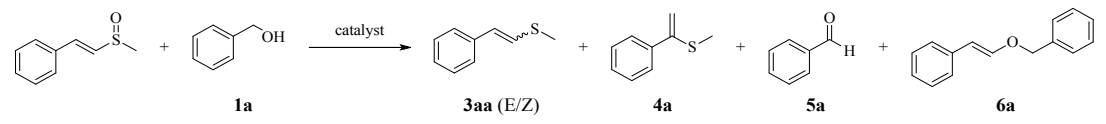
Entry	Catalyst	1a (mmol)	DMSO (mmol)	Conversion of styryl sulfoxide (%)	Yield of 3aa (E/Z) (%) ^c	Yield of 4a (%)
1	Blank	0	0	N.R.	N.D.	N.D.
2	Co@NCNT- 800	0	0	N.R.	N.D.	N.D.
3	Blank	1	0	38	21 (31/69)	5
4	Co@NCNT- 800	1	0	96	63 (24/76)	4
5	Co@NCNT- 800	0	3	N.R.	N.D.	N.D.
6	Co@NCNT- 800	0	0	21	20 (98/2)	N.D.

^a Reaction conditions: Co@NCNT-800 20 mg (9 mol% Co), styryl sulfoxide 0.5 mmol, **1a** 1 mmol, DMSO 3 mmol, KO^tBu 22.4 mg, toluene 2 mL, N₂, 160 °C, 12 h. ^b The yields was based on GC with dodecane as internal standard. ^c Yield of **3aa** was calculated based on the conversion of styryl sulfoxide. N.R.: no reaction, ND: not detected.

4.4.8 Identification of the reduction of styryl sulfoxide in a non-radical pathway

As demonstrated, TEMPO could inhibit the formation of **3aa** from coupling of **1a** and DMSO, while DPE had almost no significant effect on this reaction. We also deduced that styryl sulfoxide was a vital intermediate for the titled reaction by carefully monitoring the reaction at a short reaction time. We next performed a control experiment by using styryl sulfoxide as a starting substrate in the presence of TEMPO or DPE. The catalytic results were shown in **Table S12**. To our surprise, no conversion of styryl sulfoxide is observed with TEMPO as the additive, indicating that TEMPO can completely inhibit this reaction at the present stage. Note that 53.1% of **1a** was consumed and partially oxidized by TEMPO into **5a** (24% of yield). By contrast, as for the DPE system, we obtained 79% of styryl sulfoxide conversion with 55% of **3aa** yield, which is almost the same with the reaction without any additive. At the same time, **1a** was oxidized to **5a** with a selectivity of 87%. All these results confirm that the conversion of styryl sulfoxide is undergoing a non-radical pathway. Moreover, we are convinced that the oxidizing agents such as BQ, TEMPO and O₂ can prevent the reduction of styryl sulfoxide by benzyl alcohol to form **3aa**.

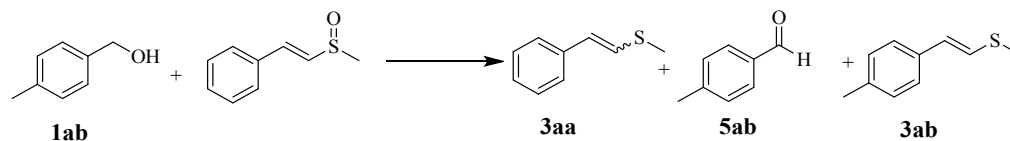
Table S12. Effect of TEMPO or DPE on the conversion of styryl sulfide^{a,b}.



Entry	Additive	Conversion of styryl sulfoxide (%)	Yield of 3aa (E/Z) (%) ^c	Conversion of 1a (%)	Yield of 4a (%)	Yield of 5a (%) ^c	Yield of 6a (%) ^c
1	TEMPO	0	0	53	0	24	-
2	DPE	79	55 (39/61)	66	5	58	8
3	no	96	63 (24/76)	38	4	35	18

^a Reaction conditions: Co@NCNT-800 20 mg (9 mol% Co), **1a** 1 mmol, styryl sulfoxide 0.5 mmol, KO^tBu 22.4 mg, toluene 2 mL, N₂, 160 °C, 12 h. ^b The yields was based on GC with dodecane as internal standard. ^c The yield of **5a** was based on the conversion of **1a** while yield of **3aa** and **6a** was based on the conversion of styryl sulfoxide.

Table S13 Control experiments of the reaction of styryl sulfoxide with 4-methyl benzyl alcohol in the presence/absence of DMSO^{a,b}.



Entry	Additive	Conversion of styryl sulfoxide (%)	Yield of 3aa (E/Z) (%) ^c	Conversion of 1ab (%)	Yield of 5ab (%) ^c	Yield of 3ab (E/Z) (%) ^c
1	-	87	58 (22/78)	83	67	-
2	DMSO	94	55 (79/21)	64	50	8 (88/12)

^a Reaction conditions: Co@NCNT-800 20 mg (9 mol% Co), **1ab** 0.5 mmol, styryl sulfoxide 0.5 mmol, KO^tBu 22.4 mg, toluene 2 mL, N₂, 160 °C, 12 h. ^b The yields was based on GC with dodecane as internal standard. ^c The yield of **3aa** was based on the conversion of styryl sulfoxide, yield of **3ab** and **5ab** was based on the conversion of **1ab**.

To better understand the reduction process of styryl sulfoxide, we next used 4-methyl benzyl alcohol as a starting substrate instead of the benzyl alcohol for this step reaction. As expected, 4-methyl benzyl alcohol (**1ab**) could reduce styryl sulfoxide to styryl sulfide (**3aa**), similar to the case of benzyl alcohol. During the reaction, 4-methyl benzyl alcohol was dehydrogenated to 4-methyl benzaldehyde. When DMSO was further introduced into the system, we obtained both styryl sulfide (**3aa**) and 4-methyl styryl sulfide (**3ab**) as the desired dehydrogenative coupling products. These results greatly supported our proposed reaction cycle.

4.5 Characterization of the used catalyst using TEM and XRD

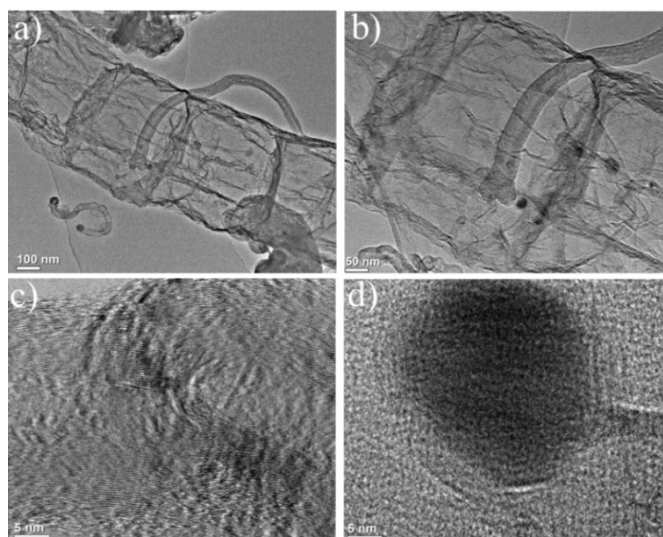


Figure S9 a, b) TEM and c, d) HR-TEM images of Co@NCNT-800 after recycle test.

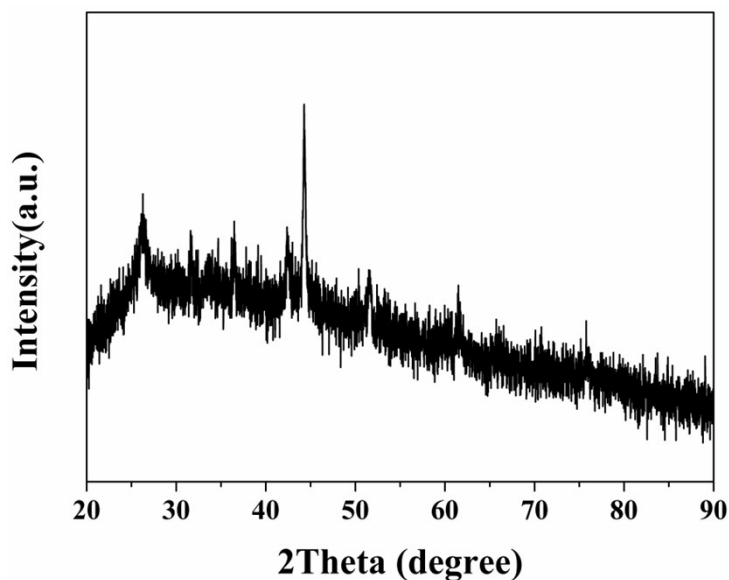


Figure S10 XRD pattern of Co@NCNT-800 after recycle test.

Post-analysis by using TEM further revealed that bamboo-like NCNTs were retained during the reaction (**Figure S9**). And XRD suggested the main Co species was still in metallic state (**Figure S10**). All these results clearly demonstrate the good stability of the Co@NCNT-800 catalyst.

4.6 The procedure for the synthesis of intermediate

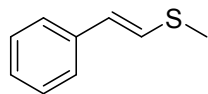
Styryl sulfoxide was prepared according to the previous literature¹⁻². In a typical reaction, a mixture of benzaldehyde (530 mg, 5 mmol), potassium hydroxide (280 mg, 5 mmol), and DMSO (10 mL) was added into a 50 mL Schlenk tube under the protection of N₂. The resulting solution was stirred at 60 °C for 1.5 h. Then the reaction was stopped and cooled down to room temperature. The saturated NaCl

aqueous (25 mL) solution was added into above system. The pH of the solution was adjusted by using 0.1 M HCl to 7.0. The solution was extracted by ethyl acetate (20 mL, 5 times) and the combined organic layers were collected and then dried by anhydrous Na₂SO₄. Finally, the solvent was removed through a rotary evaporator and the residue was purified with flash chromatography (silica gel, volume ratio of ethyl acetate to petroleum ether = 4:1) to afford the white product (233 mg, 22% yield).

5. References

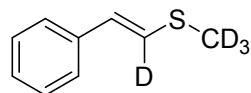
1. Zhang, Q.; Cai, S.; Li, L.; Chen, Y.; Rong, H.; Niu, Z.; Liu, J.; He, W.; Li, Y. *ACS Catal.* 2013, **3**, 1681-1684.
2. Yang, K.; Song, Q. *Org. Biomol. Chem.* 2015, **13**, 2267-2272.

6. NMR spectra

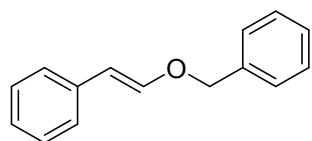


^1H NMR (400 MHz, CDCl_3) δ 6.87 (d, $J = 15.3$ Hz, 1H), 6.38 (d, $J = 15.2$ Hz, 1H).

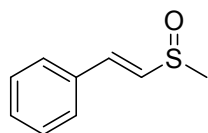
^{13}C NMR (100 MHz, CDCl_3) δ 136.97, 128.51, 126.51, 125.65, 125.23, 124.47, 116.62, 14.64.



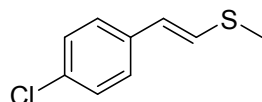
^1H NMR (400 MHz, CDCl_3) δ 7.32 (d, $J = 4.3$ Hz, 5H), 7.21 (dq, $J = 8.7, 4.2$ Hz, 1H), 6.31 (s, 1H). ^{13}C NMR (100 MHz, CDCl_3) δ 137.00, 128.57, 126.55, 125.27, 124.31, 14.18.



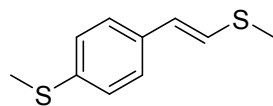
^1H NMR (400 MHz, CDCl_3) δ 7.39-7.31 (m, 5H), 7.27-7.21 (m, 4H), 7.15-7.11 (m, 1H), 7.08 (d, $J = 12.9$ Hz, 1H), 5.96 (d, $J = 12.9$ Hz, 1H), 4.90 (s, 2H). ^{13}C NMR (100 MHz, CDCl_3) δ 147.8, 136.9, 136.4, 128.7, 128.2, 127.8, 125.9, 125.3, 107.0, 72.0.



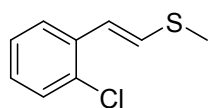
^1H NMR (400 MHz, CDCl_3) δ 7.41 – 7.35 (m, 2H), 7.33 – 7.25 (m, 3H), 7.16 (d, $J = 15.5$ Hz, 1H), 6.82 (d, $J = 15.5$ Hz, 1H), 2.60 (s, 3H). ^{13}C NMR (100 MHz, CDCl_3) δ 136.36, 133.70, 132.21, 129.77, 128.96, 127.67, 40.93.



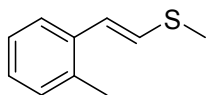
^1H NMR (400 MHz, CDCl_3) δ 7.27-7.20 (m, 4H), 6.78 (d, $J = 15.5$ Hz, 1H), 6.24 (d, $J = 15.5$ Hz, 1H), 2.38 (s, 3H). ^{13}C NMR (100 MHz, CDCl_3) δ 135.8, 132.3, 128.9, 126.9, 126.7, 123.4, 14.9.



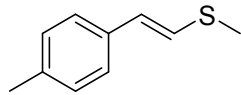
^1H NMR (400 MHz, CDCl_3) δ 7.22 – 7.16 (m, 4H), 6.74 (d, $J = 15.4$, 1H), 6.25 (d, $J = 15.4$, 1H), 2.46 (s, 1H), 2.37 (d, $J = 3.5$ Hz, 1H). ^{13}C NMR (100 MHz, CDCl_3) δ 136.6, 134.3, 127.0, 125.9, 125.4, 124.2, 16.08, 15.0.



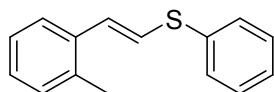
^1H NMR (400 MHz, CDCl_3) δ 7.44 (dd, $J = 7.8$ Hz, 1.2 Hz, 1H), 7.33 (dd, $J = 7.9$ Hz, 0.92 Hz, 1H), 7.22-7.18 (m, 1H), 7.14-7.10 (m, 1H), 6.84 (d, $J = 15.4$ Hz, 1H), 6.65 (d, $J = 15.4$ Hz, 1H), 2.42 (s, 1H). ^{13}C NMR (100 MHz, CDCl_3) δ 135.2, 132.0, 129.9, 129.0, 127.7, 127.0, 126.0, 120.4, 14.8.



^1H NMR (400 MHz, CDCl_3) δ 7.37 (d, $J = 7.2$ Hz, 1H), 7.18 – 7.12 (m, 3H), 6.69 (d, $J = 15.3$ Hz, 1H), 6.52 (d, $J = 15.3$ Hz, 1H), 2.41 (s, 1H), 2.35 (s, 1H). ^{13}C NMR (100 MHz, CDCl_3) δ 136.3, 134.5, 130.4, 127.0, 126.9, 126.3, 125.0, 123.0, 20.0, 15.2.



^1H NMR (400 MHz, CDCl_3) δ 7.20 (d, $J = 8.1$ Hz, 2H), 7.11 (d, $J = 8.0$ Hz, 2H), 6.73 (d, $J = 15.4$ Hz, 1H), 6.30 (d, $J = 15.4$ Hz, 1H), 2.38 (s, 3H), 2.32 (s, 3H). ^{13}C NMR (100 MHz, CDCl_3) δ 136.6, 134.5, 129.5, 125.4, 125.0, 124.7, 21.3, 15.0.



^1H NMR (400 MHz, CDCl_3) δ 7.35-7.33 (m, 3H), 7.28-7.22 (m, 2H), 7.20-7.16 (m, 1H), 7.15-7.08 (m, 3H), 6.90 (d, $J = 15.4$ Hz, 1H), 6.71 (d, $J = 15.4$ Hz, 1H), 2.26 (s, 3H). ^{13}C NMR (100 MHz, CDCl_3) δ 135.7, 135.6, 135.3, 130.6, 130.2, 129.7, 129.3, 127.8, 127.0, 126.3, 125.4, 124.4, 20.0.

